

Shapes of ellipsoidal bubbles in infinite stagnant liquids



S. Aoyama, K. Hayashi, S. Hosokawa, A. Tomiyama*

Graduate School of Engineering, Kobe University, 1-1, Rokkodai, Nada, Kobe 657-8501, Japan

ARTICLE INFO

Article history:

Received 3 June 2015

Revised 1 September 2015

Accepted 12 October 2015

Available online 30 October 2015

Keywords:

Bubble

Shape

Aspect ratio

Correlation

ABSTRACT

Aspect ratios E of ellipsoidal bubbles in infinite stagnant clean liquids are measured for $\log M = -6.6, -5.5, -4.9$ and -3.9 , where M is the Morton number. An empirical correlation of E applicable to a wide range of the Morton number is proposed by making use of the present data and Sugihara's data at $\log M = -11$ (2007). The aspect ratio in this correlation is expressed in terms of the combination of the Eötvös number and the bubble Reynolds number to account for the effects of the inertial, viscous, buoyant and surface tension forces on E . Terminal velocities of ellipsoidal bubbles are accurately predicted by using the proposed correlation and a drag correlation proposed by Rastello et al. (2011).

© 2015 Elsevier Ltd. All rights reserved.

Introduction

The shape of a bubble is one of the most important factors affecting bubble motion and heat and mass transfer from the bubble (Clift et al., 1978). The shape of a free rising bubble in an infinite stagnant liquid is known to depend on the bubble Reynolds number Re , the Eötvös number Eu and the Morton number M . Grace et al. (1976) proposed a graphical correlation of Re and the bubble shape in terms of Eu and M for $10^{-2} < Eu < 10^3$, $10^{-14} < M < 10^8$ and $10^{-1} < Re < 10^5$. Bubble shapes appearing in these ranges are spherical, ellipsoidal, wobbling, dimpled ellipsoidal-cap, skirted and spherical-cap.

The shape of an ellipsoidal bubble is characterized by the aspect ratio, E , which is the ratio of the maximum vertical dimension to the maximum horizontal dimension. Forces acting on a bubble such as the drag, lift and virtual mass forces have often been expressed in terms of E . Moore (1965) derived a drag coefficient C_D of an ellipsoidal bubble in the viscous force dominant regime in terms of Re and E . Tomiyama et al. (2002a) and Tomiyama (2004) also proposed a C_D model for bubbles in the surface tension dominant regime in terms of Eu and E . Tomiyama et al. (2002b) confirmed that the lift coefficient of a bubble is positive when the bubble is small and spherical, whereas it decreases to a negative value as E decreases with increasing the bubble diameter. It is well known that the virtual mass coefficient of a sphere is $1/2$. The virtual mass coefficient of an ellipsoidal bubble is however given as a tensor, of which the components are functions of E (Lamb, 1932; Tomiyama, 2004). The aspect ratio also plays an important role in the heat and mass transfer, e.g. the mass transfer

coefficient of an ellipsoidal bubble is expressed in terms of E , Re and the Schmidt number (Lochiel and Calderbank, 1964).

The knowledge on E is therefore of great importance in evaluating forces acting on a bubble and heat and mass transfer coefficients as well. Many studies on E have been carried out so far (Tadaki and Maeda, 1961; Moore, 1965; Wellek et al., 1966; Vakrushev and Efremov, 1970; Fan and Tsuchiya, 1990; Duineveld 1995; Kushch et al., 2002; Okawa et al., 2003; Myint et al., 2007; Sugihara et al., 2007; Legendre et al., 2012; Liu et al., 2015). Moore (1965) derived a model of E , which is a simple function of the bubble Weber number We , for bubbles of small deformation. Sugihara et al. (2007) measured bubble shapes in super-purified water and extended Moore's model so as to be applicable to bubbles of $0.5 < E < 1$. These two correlations were however proposed for bubbles in low viscosity systems and viscous effects were not taken into account. Legendre et al. (2012) carried out experiments on ellipsoidal bubbles rising through viscous liquids. They extended the Moore model by introducing a factor of M to account for the viscous effect on bubble shape. Liu et al. (2015) recently measured bubble aspect ratios for $10^{-4} < M < 10^1$ and $M = 10^{-11}$. They examined several combinations of relevant dimensionless groups for correlating E . The database of E in viscous liquids are however still insufficient, and the validity of the above correlations has not been examined sufficiently.

Shapes of single bubbles rising through infinite stagnant clean liquids were measured in this study for $10^{-7} < M < 10^{-3}$. The applicability of available correlations of E to the present data was examined. Then a correlation of E accounting for the viscous effect was proposed. The proposed correlation was applied to evaluate the bubble terminal velocity by combining the drag correlation proposed by Rastello et al. (2011).

* Corresponding author. Tel./fax: +81 78 803 6131.

E-mail address: tomiyama@mech.kobe-u.ac.jp (A. Tomiyama).

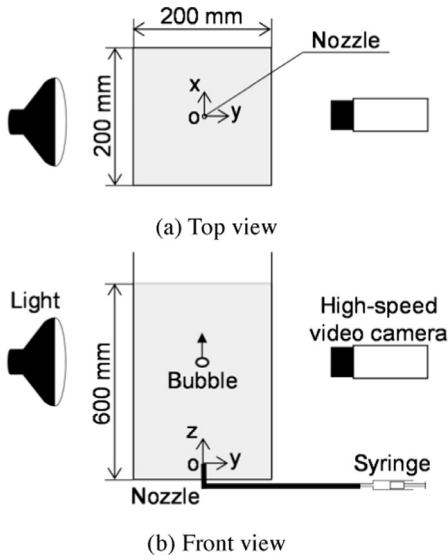


Fig. 1. Experimental setup (a) Top view, (b) Front view.

Table 1
Fluid properties at 25 °C.

$\log M$	Glycerol concentration [wt.%]	ρ_L [kg/m ³]	μ_L [Pa s]	ρ_G [kg/m ³]	μ_G [Pa s]	σ [N/m]
-6.6	62	1155	0.0098	1.2	1.8×10^{-5}	0.0670
-5.5	70	1178	0.018	1.2	1.8×10^{-5}	0.0667
-4.9	75	1191	0.026	1.2	1.8×10^{-5}	0.0666
-3.9	80	1204	0.045	1.2	1.8×10^{-5}	0.0662

Experimental

Experimental setup

Fig. 1 shows the experimental setup. The width, depth and height of the tank made of transparent acrylic resin were 0.20, 0.20 and 0.63 m, respectively. The maximum bubble diameter in the present experiment was 6.11 mm. The tank size was therefore large enough to make the wall effect on the bubble motion and shape negligible (Clift et al., 1978).

Air and glycerol–water solutions were used for the gas and liquid phases, respectively. Water purified by a Millipore system (Elix 3) and clean glycerol (Kishida-Kagaku) were used for the glycerol–water solutions. The experiments were carried out at room temperature and atmospheric pressure. The liquid density and viscosity were measured using a densimeter (Ando Keiki Co., Ltd., JIS B7525) and a viscometer (A&D, SV-10), respectively. The surface tension was measured using capillary tubes. The liquid temperature was kept at 25 ± 0.5 °C. The liquid temperature was measured using a thermometer (Netsuken, SN3000) during the experiments. The uncertainties in the measured density, viscosity and surface tension estimated at 95% confidence were 0.01%, 1.3% and 2.3%, respectively.

Table 1 shows the fluid properties of glycerol–water solutions, where M is the Morton number defined by

$$M = \frac{\mu_L^4 \Delta \rho g}{\rho_L^2 \sigma^3} \quad (1)$$

where g is the acceleration of gravity, μ the viscosity, ρ the density, σ the surface tension, $\Delta \rho$ the density difference $\rho_L - \rho_G$, and the subscripts L and G denote the liquid and the gas phases, respectively.

Single bubbles were released from the nozzle tip by injecting air from the syringe. The inner diameter of the nozzle was varied from 0.51 to 2.84 mm to form single bubbles of various sizes, which

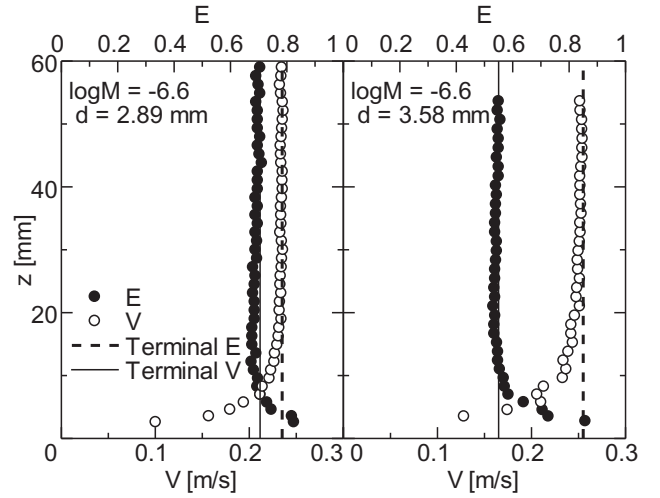


Fig. 2. Evolution of E and rising velocity V after bubble release.

resulted in $0.76 \leq d \leq 6.11$ mm, where d is the sphere-volume-equivalent bubble diameter. All bubbles in the experiments rose rectilinearly and their shapes were axisymmetric. Successive images of the bubbles were taken by using a high-speed video camera (Integrated Design Tools, M5; exposure time: 1/10,000 s, frame rate: 170 frames/s). The spatial resolution was varied from 0.63×10^{-2} to 1.07×10^{-2} mm/pixel, so that the number of pixels for d of the minimum bubble was 80.

The bubble diameters d , the bubble aspect ratios E and the bubble rising velocities V_T under terminal conditions were obtained by using an image processing method described in the following section. Examples of the measured aspect ratios and bubble rising velocities at $\log M = -6.6$ are shown in Fig. 2, where z is the vertical distance measured from the nozzle tip. In this lowest liquid viscosity system, the time constant of bubble rising motion was the largest in the fluid systems tested. The bubbles reached their terminal conditions at elevations less than 50 mm. Bubble images were therefore taken at 200 mm above the nozzle tip to assure that all the bubbles were in their terminal conditions. To check the axial symmetry of bubbles, an additional high-speed video camera was used to take their side images. Small differences between d and E calculated from the front and side images, i.e. less than 0.60% and 1.1% for d and E , confirmed that the bubbles were axisymmetric. The uncertainties in d , E and V_T estimated at 95% confidence were 1.5%, 2.5% and 0.89%, respectively.

Image processing

Detection of bubble interface

Images in the absence of bubbles were taken as background images before each measurement. The background subtraction was applied to each bubble image to clearly detect the bubble interface as shown in Fig. 3(a) and (b). The images after subtraction were transformed into binary images (Fig. 3(c)). The threshold of binarization was determined with the discriminant analysis method (Otsu, 1980). The interface was then detected by using a border following method and the pixels inside the bubble were filled up with a single color (Fig. 3(d)).

Calculation of geometric center of bubble image

The coordinates, $\mathbf{G} = (g_x(t), g_z(t))$, of the geometric center of the bubble image were calculated by

$$\mathbf{G} = \frac{\sum_{i=1}^m \sum_{k=1}^m \mathbf{r}_{i,k} \phi_{i,k}}{\sum_{i=1}^m \sum_{k=1}^m \phi_{i,k}} \quad (2)$$

Download English Version:

<https://daneshyari.com/en/article/667054>

Download Persian Version:

<https://daneshyari.com/article/667054>

[Daneshyari.com](https://daneshyari.com)